Journal of Alloys and Compounds 656 (2016) 416–422

Contents lists available at ScienceDirect

Journal of Alloys and Compounds

journal homepage: http://www.elsevier.com/locate/jalcom

A novel method for production of foamy core@compact shell Ti6Al4V bone-like composite

Shahab Ahmadi, S.K. Sadrnezhaad*

Department of Materials Science and Engineering, Sharif University of Technology, PO Box 11365-9466, Tehran, Iran

ARTICLE INFO

Article history:
Received 11 December 2014
Received in revised form
2 September 2015
Accepted 28 September 2015
Available online 1 October 2015

Keywords:
Foamy core
Compact shell
Ti6Al4V
Bone-like
Composite

ABSTRACT

This paper presents a novel method for fabrication of bone-like Ti6Al4V foamy core@compact shell composite for utilization as substitutive implant for cortical bone having porous core. Seven prototypes with core-diameters of 0, 6, 8, 10, 12, 14 and 16 mm surrounded by dense shells of respective thicknesses 8, 5, 4, 3, 2, 1 and 0 were produced by an innovative two-stage packing/compaction sintering method. Density, porosity, Young's modulus and compression strength of the prototypes depended on the core diameter. Mechanical strength and Young's modulus of 10@16 (10 mm core, 16 mm diameter prototypes) resembled that of the human ulna bone. Creation of foam at the center was achieved by carbamide powder space holder. Sintering potential model of porous spaces was a basis for heat treatment. Yield strength and Young's modulus of the prototypes ranged from 501 MPa to 46 GPa in the compact shells and 7 MPa to 2 GPa in the foamy cores of the composite samples. Final products contained 8–65% porosity with 1.45–2.84 g/cm^3 theoretical density which were within the range of the real human bone.

1. Introduction

Titanium based foams are widely used as hard tissue implants due to suitable specific strength, excellent corrosion resistance and good osseointegration [1–4]. In order to fabricate porous structures, previous investigators have used powder metallurgical and space holder techniques with sodium chloride [5–8], ammonium hydrogen carbonate [9], magnesium powder [10], polymer granules [11–13], starch [14], carbamide [15,16] and steel wires [17,18] for foam production. Studies on the effect of size and shape [19–21] and the amount of porosity [22] on properties of the products have been made.

Kim et al. [23] have used a multiple electro-discharging method for fabrication of Ti hybrid compacts consisting of solid core and porous outer shell. Poor controllability of porosity and pore-size plus high process expense are two shortcomings of this method. Lim et al. [24] have used powder metallurgical method for production of specimens having dense core and porous shell. They used Ti6Al4V alloy wires as dense core and space holder for production of the porous outer layer. Their results showed that implant compacts with porous-shells had much higher compressive strength than human bones; while the sudden change from solid core to the porous shell caused stress concentration at the core|-shell interface. In general, fully dense core of these samples developed stress shielding complications. Noncompliance with the real bone structure was another undeniable problem of these methods.

Most previous works have been focused on fabrication methods, sub-features (pore size and shape) and porosity within a simple uniform media, regardless of the actual bone bilayer structure. No studies have been found to match the exact bone structure. While it is obvious that each bone configuration definitely plays a key role in properties and implications of the biological implants. Our aim has thus been defined to study the design and manufacture of a bone-like configuration with foamy cores of different diameters surrounded by compact shells. The prototypes are to play the role of a spongy cortical bone with consolidated surface layer. The method of fabrication of foamy core@compact shell Ti6Al4V alloy is firstly devised and the mechanical behavior of the produced samples is then evaluated.

2. Experimental procedure

Sieved carbamide powders of 250–500 μm supplied by Merck KGaA were employed as space holder. Ti6Al4V milled powders (<63 μm) produced from fillings of Ti6Al4V ELI (TIMET Ltd., USA)

* Corresponding author.
E-mail address: sadrnezh@sharif.edu (S.K. Sadrnezhaad).

http://dx.doi.org/10.1016/j.jallcom.2015.09.248
0925-8388/

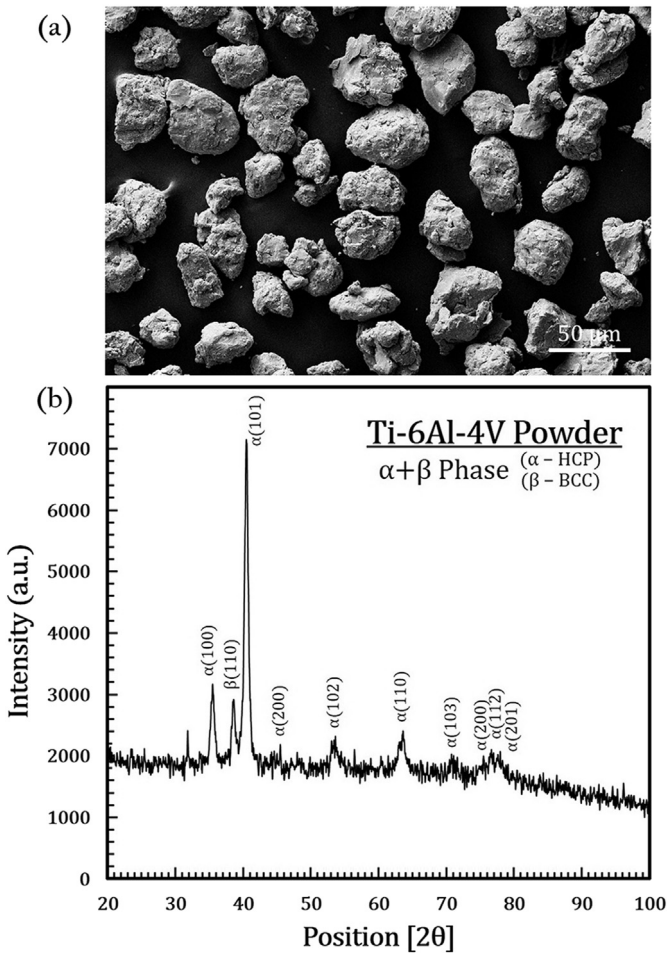

Fig. 1. Ti6Al4V powder produced by high-speed ball milling of filings made from Ti6Al4V Grade 5 rod: (a) FE-SEM image and (b) XRD pattern.

rods were used as base material. Fig. 1a shows the field emission scanning electron microscope (FE-SEM) image and Fig. 1b the X-ray diffraction pattern of the milled Ti6Al4V powder used in this research.

Mixture of Ti6Al4V and carbamide particles were cold pressed at 5 MPa into smaller diameter dies to produce foamy core green compacts. The prepared compact was placed in center of the biggest die (16 mm) and around it was filled with pure Ti6Al4V powder. High pressure (500 MPa) cold press was used to produce a 16 × 12.8 (diameter × height) mm green specimen based on the standard compression test of metallic materials at the room temperature (E9-89a, ASTM). Fig. 2 shows the procedure, schematically.

Temperature was raised from room temperature to 200 °C with a rate of 3 °C/min slow enough to avoid sudden evaporation of the space holder and possible destruction of the cell walls. The temperature was then increased under 10^{-5} torr vacuum pressure to 1200 °C and held constant for 3 h for sintering of the samples without any undesirable alloy oxidation.

Archimedes' principle was utilized to determine density and porosity of the samples. The sample was immersed into the boiling paraffin (120 °C) for 2 h for liquid paraffin impregnation of the open pores. Morphologies of the core@shell structures were inspected by scanning electron microscopy (ΣIGMA/VP ZEISS). Compression tests were carried out with universal testing machine (SANTAM STM-150, Iran) of 15 kN capacity at a crosshead speed of 0.2 mm/min. Yield strengths and elastic moduli of the porous samples were determined using 0.2%-offset method and from curves fitted to the linear elastic regions of the stress–strain curves.

3. Results and discussion

Sintering is known as the most important manufacturing step of powder metallurgy method which affects the shrinkage of the samples. It depends on temperature, time, heating rate, cooling conditions and possible phase transformation processes. Since prepared green samples contained both Ti6Al4V metallic powder and carbamide grains which had different heat behaviors, a two-

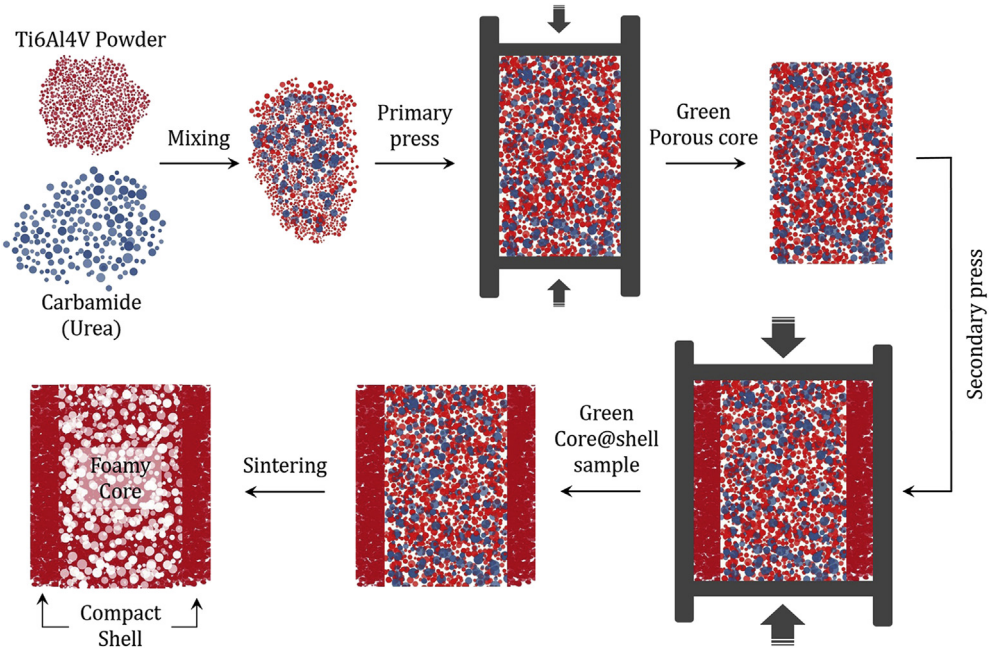

Fig. 2. Procedure for manufacturing of the foamy core@compact shell Ti6Al4V bone-like sample: (1) mixing the powders, (2) primary cold press of the inside cylinder, (3) placing green core compacts in the largest die, (4) secondary cold press at 500 MPa and (5) heating the green sample to remove the space holder and to consolidate the specimen. (For interpretation of the references to color in this figure legend, the reader is referred to the web version of this article.)

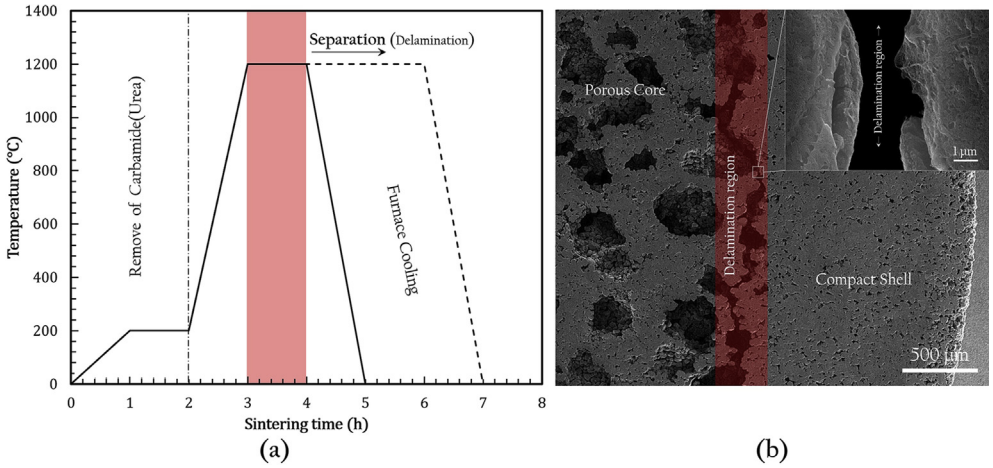

Fig. 3. (a) Heat treatment steps of Ti6Al4V foamy core@compact shell samples: (i) initial step is related to carbamide removal and (ii) Ti6Al4V powder sintering at higher temperatures. Separation of porous core from compact shell occurs when the sample is held at 1200 °C for longer than 1 h. (b) FE-SEM micrograph of foamy core@compact shell sample sintered at 1200 °C for 3 h. More shrinkage of porous core compared to the compact shell in too long a sintering time causes delamination at the core|shell interface.

step heat treatment procedure was deduced for removal of carbamide particles (1st step) and sintering of the titanium alloy powders (2nd step). Based on differential thermal analysis of carbamide and sintered Ti6Al4V powders, heat treatment procedure used in this research included the following two steps: (1) 1 h at 200 °C for removal of carbamide and (2) 3 h at 1200 °C followed by furnace cooling. In this step, sintering of titanium occurs. It has also been used by previous authors [16,19,25,26] to assure good connection of Ti6Al4V particles together. Experimental results primarily showed that separation (delamination) of the porous core from the compact shell accompanied with considerable core shrinkage under this condition. FE-SEM micrograph inspection showed that excessive holding time of 3 h at 1200 °C caused delamination of the heterogeneous regions, as illustrated in Fig. 3.

Separation of porous core from dense shell is a major drawback in bilayer prototype manufacturing. Based on the investigations already conducted by Cocks [27], it is understood that the difference in the pore size of the core and the shell regions is the main cause of difference in the sintering and shrinkage rates. The Gibbs free energy change of the regions containing spherical pores can be evaluated by Ref. [27]:

$$dG = \left[\frac{2\gamma_s(1-cos\theta)}{r} - \Sigma_m\right]dV \quad (1)$$

where dG is Gibbs free energy change, dV is volume change, γs is the surface tension, θ is half of the dihedral angel, Σ_m is the mean stress and r is the pore radius. Since spherical pore volume increases by the following arbitrary amount:

$$dV = rdA/2 \quad (2)$$

dG can only be negative when [27].

$$\Sigma_m \geq \frac{2\gamma_s(1-cos\theta)}{r} = \Sigma_s \quad (3)$$

where Σ_s is the sintering potential which only depends on the size of the large pores while it is independent of the grain size and the other factors responsible to the densification mechanisms [27]. It is clear from Eq. (3) that the sintering potential is inversely proportional to the pore radius. In other words, sintering of the compact shells having small pores is faster than the cores hosting very large pores. According to the Cocks model, the compact shells are sintered before the porous cores. This means that at the same time when the porous cores are passing the shrinkage stage, the compact shells are in their final step of sintering procedure which has a slow rate. In order to have good connection between different pore size regions, sintering should be completed in a time interval (Δt) in between the time required for sintering of the mixed powders and large pore size area shrinkage.

As mentioned previously, a delamination region appears at the core|shell interfaces in case of too long a sintering time due to the

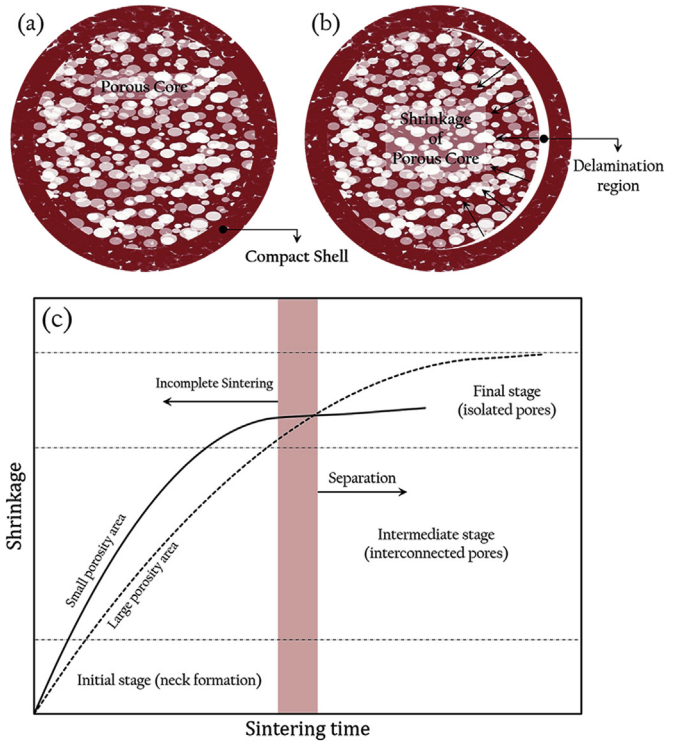

Fig. 4. Schematics of top surface of the foamy core@compact shell samples sintered for (a) proper enough and (b) too long a sintering time. (c) Proper time selection for sintering of different pore-size regions. Notice that the large-pore areas exhibit slower sintering than the small-pore regions. Appearance of the delamination region is due to higher shrinkage of porous core as compared to the compact shell because of too long a sintering time.

higher shrinkage of the porous core in comparison to the compact shell which helps reduction of the surface energy.

It is generally believed that shrinkage increases with sintering time [28]. But despite the great number of experimental and theoretical investigations carried out on bimodal porous materials shrinkage due to sintering, no accepted single opinion does exist on the influence of pore size distribution and ration on kinetics of the process.

Olevsky [29] has presented, for example, small and large pore size growth against the specific sintering time (τ):

$$\frac{dR_P}{d\tau} = \frac{R_P(1-\theta)^2}{2(\Pi-1)}\left[\frac{1+(k-1)\Pi}{3\psi}+\frac{k}{2\phi}\right] \tag{4}$$

$$\frac{dr_P}{d\tau} = -\frac{r_P}{4(1-\theta)} \tag{5}$$

$$\tau = \int_t \frac{P_L}{\eta}dt \tag{6}$$

where P_L is the Laplace pressure, η is the effective shear moduli, t is the real time of sintering, k is the ratio of small (r_p) to large (R_p) pore radii. Π is the volume fraction of large pores, φ and ψ are described by the following equations [29]:

$$\phi = (1-\theta)^2 \tag{7}$$

$$\psi = 2/3\frac{(1-\theta)^3}{\theta} \tag{8}$$

where θ is the volume ratio of the pores (V_{pores}) to the whole sample (V_{total}).

In order to determine the kinetics of the shrinkage of the porous region, quantification of fundamental parameters like Laplace pressure, effective shear moduli, θ and pore diameters are necessary. It should be noted that according to Eq. (1), the large-pore diameter increases by the sintering time which confirms a disputable theory [29]. However, Pan et al. [30] have recently found out that the large pores of a powder compact have shrunk during sintering. They have given the following equation for kinetics of shrinking of the large pores:

$$\frac{dR}{dt} = -\frac{1+\mu}{2\eta}\frac{R_1^3 p}{R_2^3-R_1^3}\frac{R_2^3}{R^2} - \frac{12\mu}{\eta}\left(\frac{R_1^3 p}{R_2^3-R_1^3}+\sigma_s\right)R \tag{9}$$

where μ represents the Poisson's ratio, η is the unidirectional viscosity of the shell matrix, σ_s is referred to as the sintering stress, R_1 and R_2 describe large pore and under-study shell material radii, R describes the radial velocity of the shell material at location R and p is the equivalent of applying traction on the surface of the large pore given by Refs. [31,32]:

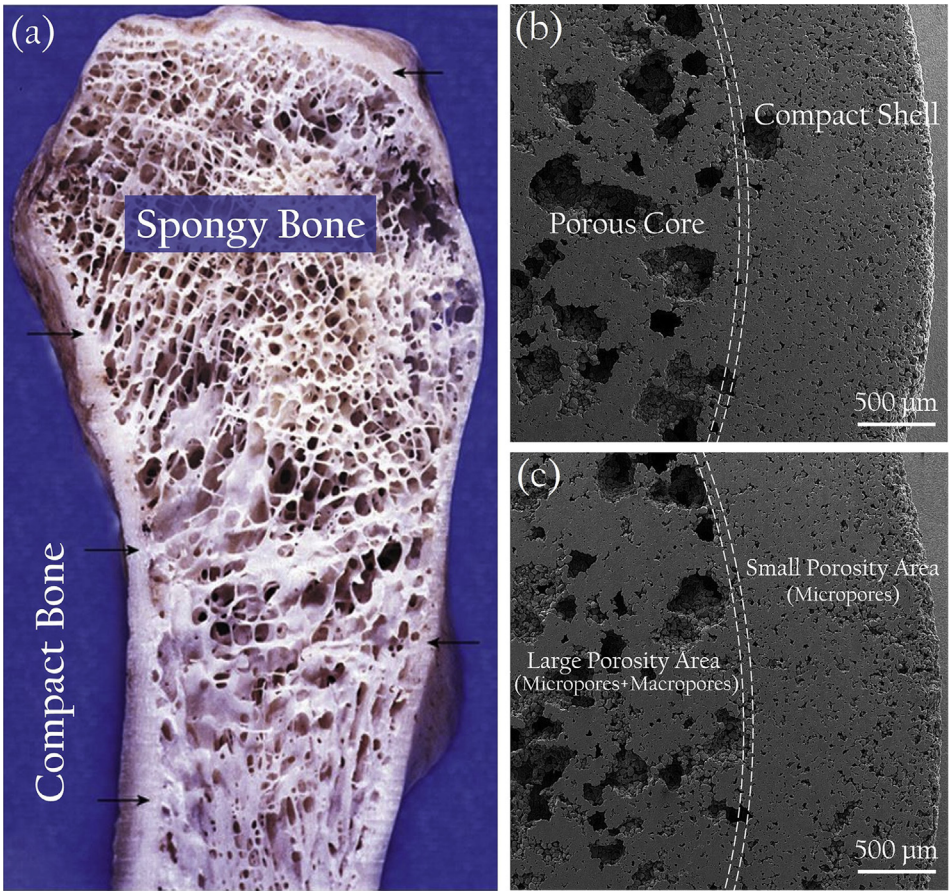

Fig. 5. (a) Epiphysis of an adult long bone [24]. (b, c) Scanning electron microscopy images of the foamy core@compact shell sample. The images illustrate two regions; (i) foamy core consisting of macro- and micro-pores and (ii) compact shell with micro-pores. The macro- and micro-pores are created due to the evaporation of carbamide grains and incomplete sintering of the sample, respectively.

$$p = 2\frac{\gamma_s}{R_1} \tag{10}$$

where γ_s is the specific surface energy. As is clear from Eq. (6), in order to evaluate kinetics of sintering to find a suitable sintering time for bimodal porous structures (such as foamy core@compact shell), quantitative measurements of some fundamental parameters such as specific surface energy, Poisson's ratio and unidirectional viscosity are essential. However, it is noteworthy that Eq. (6) shows the large pores shrinkage during sintering which means that the regions with large pores (foamy core) suffer more shrinkage than the compact sections (compact shell). However, the total shrinkage increases during the sintering [28].

At first, a long sintering time of 3 h was chosen in this research. This has usually been selected for production of titanium foam via space holder technique for assurance of good Ti6Al4V powders connection. Under this condition, a separation (delamination) between the foamy core and compact shell appears. The FE-SEM micrograph of the specimen sintered at 1200 °C for 3 h showed delamination at the core|shell interface, as shown in Fig. 3b.

There are two accepted theories concerning the delamination effect:

1. Amount of shrinkage increases during sintering [28–30].
2. The regions of different pore sizes have different sintering and shrinkage rates [27], i.e. large pore size regions observe slower sintering rates while compact structures perceive higher shrinkage rate but lower shrinkage amount.

In the following experiments, the duration of sintering was reduced step by step to control the amount of shrinkage in the foamy core@compact shell specimen. Finally, the sintering time of 1 h was selected for integration of the structure. Schematics of the samples sintered under proper and too long conditions are presented in Fig. 4a and b while the proper time interval necessary for sintering different pore size regions is presented in Fig. 4c. According to the mentioned concept, the Ti6Al4V foamy core@compact shell was heat treated at 1200 °C for 1 h.

Devising the two-step procedure used here reduced shrinkage, compensated gap production and increased layers attachment at the interface. Fig. 5b, c indicates satisfactory attachment of porous|solid layers.

A comparison is made of the epiphysis of an adult long bone with the FE-SEM image of a foamy core@compact shell sample in Fig. 5. Two regions are distinguishable in the pictures: (i) foamy core consisting of macro and micro pores and (ii) compact shell with sole micro-pores. Macropores of the Ti6Al4V samples are outcome of the carbamide evaporation. Their micro pores are resulted from incomplete sintering of the powder mixtures.

Based on morphological observations, 8–64% of the foamy core@compact shell pores were interconnected. Closer microscopic examinations revealed appropriate attachment of the sintered regions in both core and shell areas. Different interface regions showing typical neck appearance are illustrated in Fig. 6. It is interesting to note that although the porous core of the prototypes benefited from less sintering rate than their compact shell, the particles at the core areas exhibited acceptable junctions that could

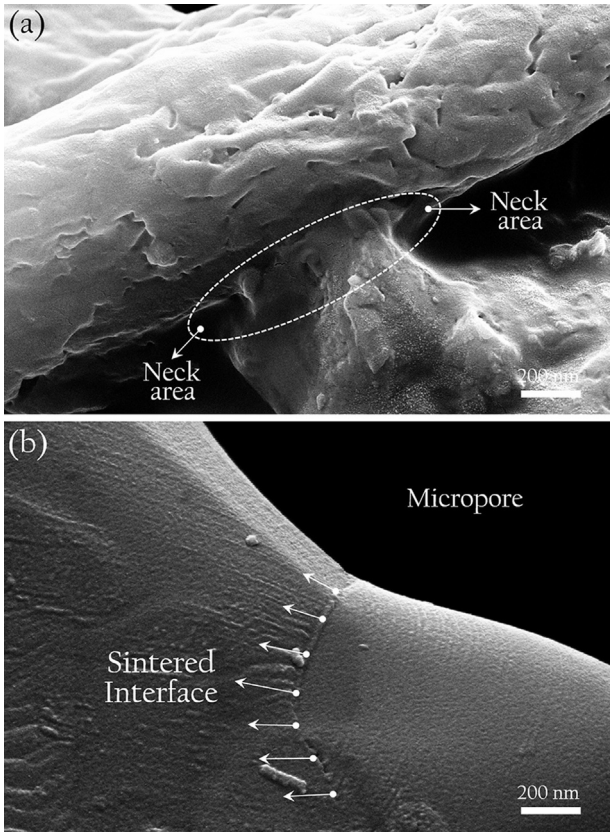

Fig. 6. FE-SEM images of the sintered areas and neck regions of: (a) porous core and (b) compact shell regions of the Ti6Al4V alloy.

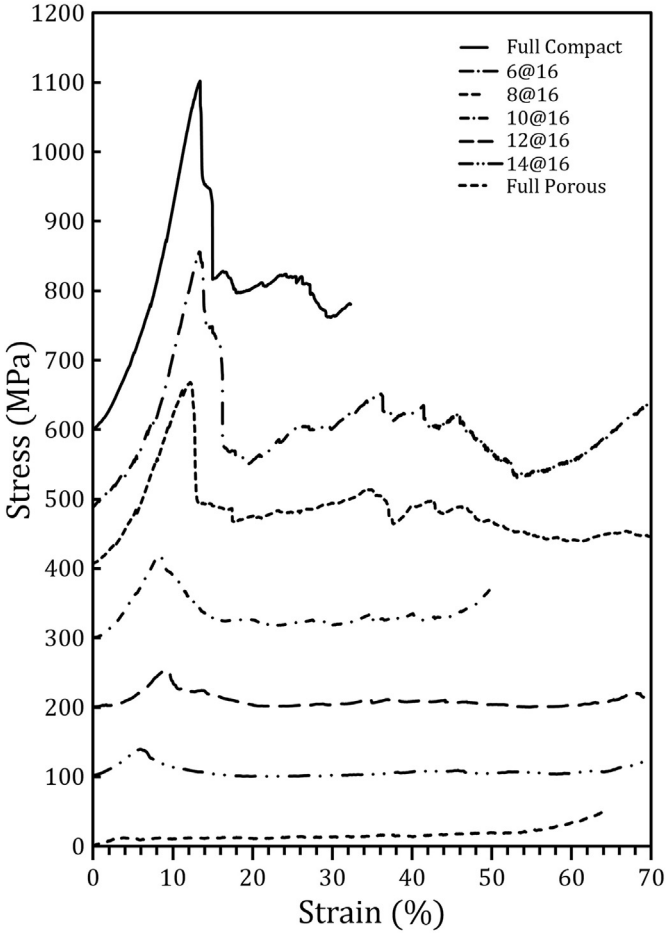

Fig. 7. Typical compression curves for foamy core@compact shell Ti6Al4V samples produced in this research. Note that each stress–strain curve is shifted 100 MPa above the lower strength curve to eliminate interferences.

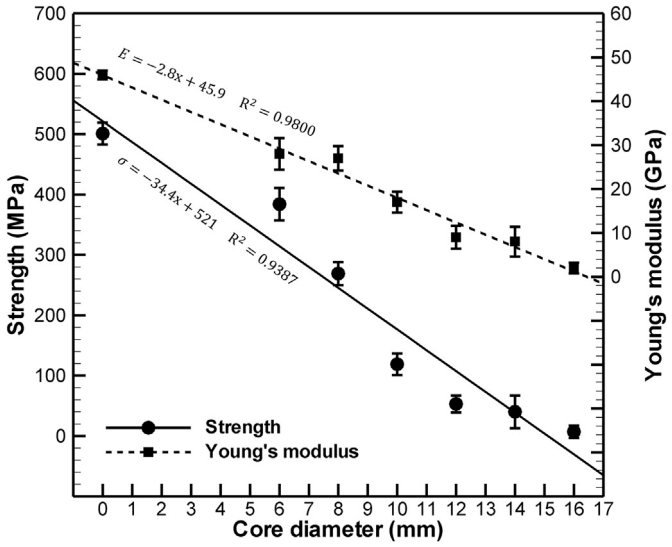

Fig. 8. Strength and Young's modulus of foamy core@compact shell Ti6Al4V against core diameter of the sample. Notice that 10@16 sample complies with the human ulna specifications [34–36].

result in strong mechanical behavior.

Fig. 7 shows the compression test results of the porous Ti6Al4V prototypes having various core diameters. As can be observed, the samples exhibit metallic foam behavior consisting of an initial elastic deformation, a wide plateau region and a final densification stage. Fig. 7 indicates yield strength reduction from 501 MPa (for dense sample) to 7 MPa (for porous sample) against the core diameter of the produced specimens. The Young's moduli of the samples decrease from 46 to 2 GPa by the foamy core diameter increase.

It is interesting to note that the mechanical characteristics of the sample manufactured with a core diameter of 10 mm (10@16) resemble the human bone [33–35]. Appropriate porosity for cell anchoring and bone growth can provide desirable consonant for minimization of problems caused by bone mismatch and strength difference. New structure should reduce stress shielding effects for long-term stabilization of implants in the patient's body. Fig. 8 plots the strength and Young's modulus of the produced samples versus foamy core diameter as compared with typical human bone specifications.

Bone replacement generally requires transfer of body fluid for in-growth of live tissue. Design and manufacturing of innovative implants emulating the structural and mechanical behavior of human bone double layer have been aimed in this research. Porous structures can fulfill these requirements plus force-displacement adjustments usually needed for elimination of implant-bone mismatch.

The bilayer foamy core@compact shell implants produced here have structural properties close to the spongy-compact bones. An obvious benefit is lessening of the stress shielding which lowers adjacent tissue damage. Previous researchers have explained bone|implant fixation and long term stabilization [37,38]. Schematics of a long bone epiphysis which has been repaired by a novel foamy core@compact shell implant is illustrated in Fig. 9.

Table 1 compares the mechanical properties of a number of foamy core@compact shell implants. Both Young's modulus and density of the implants reduce through introduction of pores in core of the samples. Interconnected highly porous cores facilitate transportation of blood and nutrients within the implant where leading to the ingrowth and fixation of the bone cells [39–41]. The

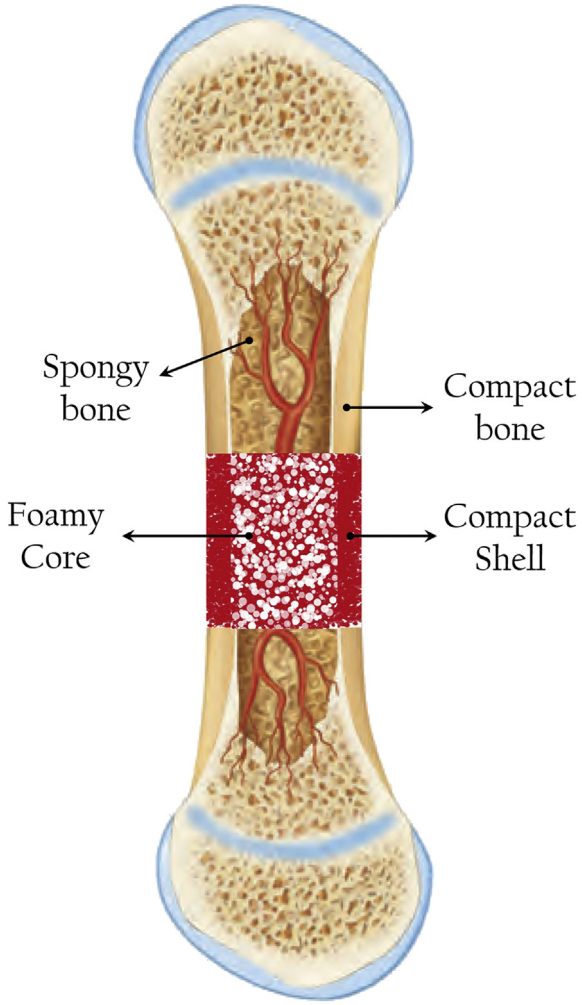

Fig. 9. Schematics of epiphysis of a long bone with spongy-compact texture repaired by a foamy core@compact shell implant.

strength of the implant is at the same time maintained around the human bone range via compact shell presence.

As is seen in Fig. 8, the sample with 10 mm core diameter totally complies with mechanical specifications of the human ulna. Yield strength, Young's modulus, density and porosity of the manufactured samples are summarized in Table 1.

Because of low sintering potential, fully porous sample (16@16) suffers from weak strength and low Young's modulus. There are other samples, however, that perform remarkably close to the human bone mechanical behavior despite the short sintering time that they need for strengthening their shell.

4. Conclusions

Foamy core@compact shell Ti6Al4V alloy prototypes were successfully fabricated via a double stage space holder technique. According to Cocks model, sintering procedures of two regions with different pore sizes were considered. It was found out that a good connection between the foamy and the condensed regions was achievable with selection of a defined time range (Δt) for sintering duration. Δt should be between the times required for sintering of the powders and when the shrinkage rate of the areas with larger pores is more than that of smaller ones. The sample made with a core diameter of 10 mm (10@16) showed similar mechanical

Table 1
Physical and mechanical properties of the manufactured foamy core@compact shell Ti6Al4V alloy samples.

Sample	Diameter (mm)	Porosity (%)	Density (g/cm^3)	Compression Young's modulus (GPa)	Compression yield strength (MPa)
1	0@16 (Compact)	8.97	2.84	46	501
2	6@16	9.32	2.33	28	384
3	8@16	15.39	2.04	27	269
4	10@16	23.85	1.97	17	119
5	12@16	27.97	1.87	9	53
6	14@16	39.78	1.74	8	40
7	16@16 (Fully porous)	64.08	1.45	2	7
Human bone [34–36]	Different tissues: Ulna to Femur	3.5–79.3	1.24–3.10	14.7–34.3	167–213

behavior to the human ulna bone that it can reduce mismatch problems to minimum and promise a long-term stabilization of the produced specimens.

Acknowledgments

Research deputy of Sharif University of Technology is appreciated for his continuous support of this research.

References

[1] Y. Okazaki, E. Nishimura, H. Nakada, K. Kobayashi, Surface analysis of Ti–15Zr–4Nb–4Ta alloy after implantation in rat tibia, Biomaterials 22 (2001) 599–607.
[2] M. Long, H.J. Rack, Titanium alloys in total joint replacement—a materials science perspective, Biomaterials 19 (1998) 1621–1639.
[3] D. Kuroda, M. Niinomi, M. Morinaga, Y. Kato, T. Yashiro, Design and mechanical properties of new β type titanium alloys for implant materials, Mater Sci. Eng. A 243 (1989) 244–249.
[4] K.H.W. Seah, R. Thampuran, S.H. Teoh, The influence of pore morphology on corrosion, Corros. Sci. 40 (1998) 547–556.
[5] N. Jha, D.P. Mondal, J. Dutta Majumdar, A. Badkul, A.K. Jha, A.K. Khare, Highly porous open cell Ti-foam using NaCl as temporary space holder through powder metallurgy route, Mater Des. 47 (2013) 810–819.
[6] Y. Torresa, J.J. Pavónb, J.A. Rodrígueza, Processing and characterization of porous titanium for implants by using NaCl as space holder, J. Mater. Process. Technol. 212 (2012) 1061–1069.
[7] Bing Ye, David C. Dunand, Titanium foams produced by solid-state replication of NaCl powders, Mater. Sci. Eng. A 528 (2010) 691–697.
[8] S.K. Sadrnezhaad, M. Aryana, N. Hassanzadeh Nemati, M. Alizadeh, A. Ebadifar, Single and double stage sintering of mechanically alloyed powder for nanostructured Ti6Al4V foams usable in cancellous scaffolds, Int. Heat Treat. Surf. Eng. 7 (2013) 43–48.
[9] Changshu Xiang, Yan Zhang, Zengfeng Li, Hanliang Zhang, Yuanping Huang, Huiping Tang, Preparation and compressive behavior of porous titanium prepared by space holder sintering process, Procedia Eng. 27 (2012) 768–774.
[10] Ziya Esen, Sakir Bor, Characterization of Ti–6Al–4V alloy foams synthesized by space holder technique, Mater. Sci. Eng. A 528 (2011) 3200–3209.
[11] C.S.Y. Jee, N. Ozguven, Z.X. Guo, J.R.G. Evans, Preparation of high porosity metal foams, Metall. Mater. Trans. B 31 (2000) 1345–1352.
[12] G. Rausch, J. Banhart, in: H.P. Degischer, B. Kriszt (Eds.), Handbook of Cellular Metals, Wiley, 2002, p. 21.
[13] B.Q. Li, F. Yan, X. Lu, Effect of microstructure on the tensile property of porous Ti produced by powder metallurgy technique, Mater. Sci. Eng. A 534 (2012) 43–52.
[14] Amirhossein Mansourighasri, N. Muhamad, A.B. Sulong, Processing titanium foams using tapioca starch as a space holder, J. Mater. Process. Technol. 212 (2012) 83–89.
[15] M. Sharma, G.K. Gupta, O.P. Modi, B.K. Prasad, Anil K. Gupta, Titanium foam through powder metallurgy route using acicular urea particles as space holder, Mater. Lett. 65 (2011) 3199–3201.
[16] Wenjuan Niu, Chenguang Bai, GuiBao Qiu, Qiang Wang, Processing and properties of porous titanium using space holder technique, Mater. Sci. Eng. A 506 (2009) 148–151.
[17] Daniel J. Jorgensen, David C. Dunand, Structure and mechanical properties of Ti–6Al–4V with a replicated network of elongated pores, Acta Mater. 59 (2011) 640–650.
[18] Daniel J. Jorgensen, David C. Dunand, Ti–6Al–4V with micro- and macropores produced by powder sintering and electrochemical dissolution of steel wires, Mater. Sci. Eng. A 527 (2010) 849–853.
[19] Byounggab Lee, Taekyung Lee, Yongmoon Lee, Dong Jun Lee, Jiwon Jeong, Junhan Yuh, Sang Ho Oh, Hyoung Seop Kim, Chong Soo Lee, Space-holder effect on designing pore structure and determining mechanical properties in porous titanium, Mater. Des. 57 (2014) 712–718.
[20] S. Naddaf Dezfuli, S.K. Sadrnezhaad, M.A. Shokrgozar, S. Bonakdar, Fabrication of biocompatible titanium scaffolds using space holder technique, J. Mater. Sci. Mater. Med. 23 (2012) 2483–2488.
[21] A. Ghasemi, S.R. Hosseini, S.K. Sadrnezhaad, Pore control in SMA NiTi scaffolds via space holder usage, Mater. Sci. Eng. C 32 (2012) 1266–1270.
[22] Amit Bandyopadhyay, Felix Espana, Vamsi Krishna Balla, Susmita Bose, Yusuke Ohgami, Neal M. Davies, Influence of porosity on mechanical properties and in vivo response of Ti6Al4V implants, Acta Biomater. 6 (2010) 1640–1648.
[23] J.H. Lee, H.J. Park, S.H. Hong, J.T. Kim, W.H. Lee, J.M. Park, K.B. Kim, Characterization and deformation behavior of Ti hybrid compacts with solid-to-porous gradient structure, Mater. Des. 60 (2014) 66–71.
[24] Montasser M. Dewidar, J.K. Limc, Properties of solid core and porous surface Ti–6Al–4V implants manufactured by powder metallurgy, J. Alloys Compd. 454 (2008) 442–446.
[25] Lucía Reiga, Vicente Amigób, David J. Busquetsb, Jose A. Caleroc, Development of porous Ti6Al4V samples by microsphere sintering, J. Mater. Process. Technol. 212 (2012) 3–7.
[26] D.S. Li, Y.P. Zhang, X. Ma, X.P. Zhang, Space-holder engineered porous NiTi shape memory alloys with improved pore characteristics and mechanical properties, J. Alloys Compd. 474 (2009) L1–L5.
[27] Alan C.F. Cocks, Constitutive modeling of powder compaction and sintering, Prog. Mater. Sci. 46 (2001) 201–229.
[28] Suk-Joong L. Kang, Sintering: Densification, Grain Growth, and Microstructure, First published, Elsevier Butterworth-Heinemann, Burlington, 2005.
[29] Eugene A. Olevsky, Theory of sintering: from discrete to continuum, Mater. Sci. Eng. R23 (1998) 41–100.
[30] Jingzhe Pan, Alan Cocks, Jurgen Rodel, Ruoyu Huang, Heok Ngee Ch'ng, Densification of powder compact containing large and small pores, J. Am. Ceram. Soc. 92 (7) (2009) 1414–1418.
[31] J. Pan, H.N. Ch'ng, A.C.F. Cocks, Sintering kinetics of large pores, Mech. Mater. 37 (2005) 705–721.
[32] J.K. Mackenzie, R. Shuttleworth, A phenomenological theory of sintering, R. Proc. Phys. Soc. Lond. Sect. B 62 (1949) 833–852.
[33] Michael H. Ross, Wojciech Pawlina, A Text and Atlas: with Correlate Cell and Molecular Biology, sixth ed., Wolters Kluwer|Lippincott Wiliams & Wilkins, 2011.
[34] G.A.P. Renders, L. Mulder, L.J. van Ruijven, T.M.G.J. van Eijden, Porosity of human mandibular condylar bone, J. Anat. 210 (3) (Mar 2007) 239–248.
[35] S. Biswas, P.C. Pramanik, P. Dasgupta, A. Chanda, Study of microstructure and mechanical properties of human cortical bone, Int. J. Sci. Eng. Res. 2 (3) (March 2011) 1–8.
[36] J.R. Caeiro, P. Gonzalez, D. Guede, Biomechanics and bone (& II): trials in different hierarchical levels of bone and alternative tools for the determination of bone strength, Rev. Osteoporosis Metab. Miner. 5 (2) (Jun. 2013) 1–13.
[37] Ik-Hyun Oh, Naoyuki Nomura, Naoya Masahashi, Shuji Hanada, Mechanical properties of porous titanium compacts prepared by powder sintering, Scr. Mater. 49 (2003) 1197–1202.
[38] R. Ricceri, P. Matteazzi, P/m processing of cellular titanium, Int. J. Powder Metall. 39 (3) (2003) 53–61.
[39] B.V. Krishna, S. Bose, A. Bandyopadhyay, Low stiffness porous Ti structures for load-bearing implants, Acta Biomater. 3 (2007) 997–1006.
[40] V. Karageorgiou, D. Kaplan, Porosity of 3D biomaterial scaffolds and osteogènesis, Biomaterials 26 (2005) 5474–5491.
[41] S. Kujalaa, J. Ryhanen, A. Danilovb, et al., Effect of porosity on the osteointegration and bone ingrowth of a weight-bearing nickel–titanium bone graft substitute, Biomaterials 24 (2003) 4691–4697.